

RESEARCH

Open Access



FGA can be used as a promising therapeutic target in osteoarthritis

Guanhong Chen¹, Han Zhang² and Xizhuang Bai^{1,3,4*}

Abstract

Background This study aims to identify critical signaling pathways and pathogenic genes involved in osteoarthritis (OA) to provide a foundation for identifying targeted therapeutic strategies.

Methods Twenty-six patients who underwent knee joint surgery in the Department of Orthopedics between January and December 2023 were enrolled. Cartilage samples in the experimental group (OA group) were harvested from the articular surfaces of the knee joints of OA patients undergoing total knee arthroplasty (TKA). In contrast, control samples were obtained from non-load-bearing regions of irreparable cartilage fragments excised during surgical management of tibial plateau fractures. Proteomic profiling was conducted using label-free quantitative mass spectrometry-based proteomics. Subsequent bioinformatics analysis was performed using R version 4.3.3 to identify differentially expressed proteins and key pathogenic genes. Quantitative real-time polymerase chain reaction (qPCR) and western blots were employed to validate the expression levels of candidate genes.

Results The proteomic analysis revealed that regulatory signaling pathway of insulin-like growth factor-binding protein (IGFBP) for IGF transport and uptake and the platelet degranulation signaling pathway were significantly implicated in OA pathogenesis. Among the differentially expressed proteins, fibrinogen alpha chain (*FGA*) was identified as a central gene associated with OA. The qPCR and western blots validation confirmed significantly elevated expression of *FGA* in OA articular chondrocytes samples compared to controls.

Conclusions *FGA* plays a pivotal role in the molecular pathology of OA and may represent a promising therapeutic target for the development of precision treatments for OA.

Keywords Osteoarthritis, Proteomic analysis, Key gene, Targeted therapy, Fibrinogen alpha chain

Background

Osteoarthritis (OA) is a chronic, degenerative joint disorder and the most prevalent musculoskeletal disease worldwide. It is characterized by progressive degradation of articular cartilage, subchondral bone remodeling, meniscal degeneration, and inflammation and fibrosis of both the infrapatellar fat pad and synovial membrane [1]. The disease imposes a substantial global health burden, with approximately 10% of men and 18% of women over the age of 60 affected [2]. In the United States alone, OA contributes to significant socioeconomic costs, accounting for an estimated 1.0–2.5% of the national gross

*Correspondence:

Xizhuang Bai
cghhgg@126.com

¹Dalian Medical University, Dalian 116041, China

²Department of Joint Surgery, The Affiliated Hospital of Qingdao University, Qingdao 266000, China

³Department of Arthrology, Liaoning Provincial People's Hospital, Shenyang 110000, China

⁴Department of Arthrology, Dalian Medical University, Liaoning Provincial People's Hospital, No. 33 Wenyi Road, Shenhe District, Shenyang City, Liaoning Province, China



© The Author(s) 2025. **Open Access** This article is licensed under a Creative Commons Attribution-NonCommercial-NoDerivatives 4.0 International License, which permits any non-commercial use, sharing, distribution and reproduction in any medium or format, as long as you give appropriate credit to the original author(s) and the source, provide a link to the Creative Commons licence, and indicate if you modified the licensed material. You do not have permission under this licence to share adapted material derived from this article or parts of it. The images or other third party material in this article are included in the article's Creative Commons licence, unless indicated otherwise in a credit line to the material. If material is not included in the article's Creative Commons licence and your intended use is not permitted by statutory regulation or exceeds the permitted use, you will need to obtain permission directly from the copyright holder. To view a copy of this licence, visit <http://creativecommons.org/licenses/by-nc-nd/4.0/>.

domestic product annually [3]. OA pathogenesis is multifactorial, driven by a combination of genetic susceptibility, aging, obesity, joint misalignment, and prior trauma or surgical interventions [4]. Genome-wide association studies (GWAS) have identified at least 11 genetic loci associated with OA, and over 80 genes are believed to contribute to its polygenic and heritable etiology [5].

At the molecular level, several signaling pathways have been involved in OA progression [6]. Inhibition of tumor growth factor (TGF)- β signaling pathway can promote the occurrence and development of OA. TGF- β binds to type II receptors and activates the typical TGF- β /Smad signaling cascade, thereby promoting chondrocyte matrix synthesis and inhibiting the hypertrophy and maturation of chondrocytes, thus playing an important role in the pathogenesis of OA and cartilage repair [7]. Similarly, the Wnt/ β -catenin signaling pathway regulates multiple developmental processes in the bones and joints, and it is also involved in the occurrence and development of OA. Overexpression of β -catenin leads to the loss of the phenotype of chicken chondrocytes, evidenced by decreased expressions of Sox9 and Col2. The Indian Hedgehog (Ihh) signaling pathway also influences chondrocyte differentiation during endochondral ossification through its negative feedback interaction with parathyroid hormone-associated protein (PTHrP) [8].

However, no effective targeted therapeutic drugs have yet exhibited clinical efficacy in regulating these signaling pathways for OA treatment. Current treatment methods for OA, including physiotherapy, complementary treatments, oral medication, intra-articular injections, and surgical intervention, are largely symptomatic. Early interventions focus on reducing pain and stiffness, whereas advanced disease management aims to preserve joint function [9]. At present, there is no specific treatment for OA in clinical practice, especially molecularly targeted therapies [10]. Therefore, we performed a proteomic analysis to identify crucial signaling pathways and key pathogenic genes involved in the pathogenesis of OA. By elucidating the molecular mechanisms, this study aims to lay the theoretical foundation for the development of targeted therapies for OA.

Materials and methods

Clinical samples

Twenty-six patients who underwent knee joint surgery at the Department of Orthopedics between January and December 2023 were selected. The experimental group (OA group) consisted of patients diagnosed with knee OA who underwent total knee arthroplasty (TKA), from whom degenerated articular cartilage was harvested during surgery. The control group comprised patients undergoing arthroscopically assisted open reduction and internal fixation (ORIF) for tibial plateau fractures.

In this group, non-load-bearing cartilage from irreparable regions was collected. All cartilage samples were obtained during surgery for subsequent proteomic analysis. Written informed consent was obtained from the patients and their families, and the study protocol was approved by the hospital's medical ethics committee on December 3, 2022 (Approval No.2022120316).

Inclusion and exclusion criteria

Patients in the experimental group were diagnosed with OA based on clinical symptoms, including joint pain, swelling, stiffness, and functional limitation, combined with X-ray findings such as joint space narrowing, osteophyte formation, and subchondral bone sclerosis. Control group patients did not exhibit any radiographic or clinical evidence of OA. The inclusion criteria for both groups were as follows: (1) No previous surgical intervention on the affected knee; (2) no contraindications to undergoing surgery; (3) absence of serious comorbid conditions such as psychiatric disorders, cardiovascular disease, or cerebrovascular disease; (4) no evidence or history of systemic inflammatory arthropathies, including rheumatoid arthritis and psoriatic arthritis. Patients who did not meet these criteria were excluded.

Reagents and consumables

Ammonium bicarbonate (Sigma-Aldrich, lot number: A6141-500G), TEAB (Sigma-Aldrich, T7408-100mL), Urea (Amresco, lot number: M123-1KG), Protein quantitative stain (Huaxingbio, lot number: HXJ5137), and Cow Albumin serum (Thermo Scientific, lot number: 23209), Disulfide DTT (Amresco, lot number: M109-5G), Iodoacetylamine IAM (Amresco, lot number: M216-30G), Trypsin (Promega, lot number: V5280/100ug), Zip-tip (Millipore, lot number: ZTC18M096), Acetonitrile (J.T.Baker, lot number: 34851 MSDS), Ammonia water (Wako Pure Chemical Industries Ltd, No.013-23355), Formic acid (Sigma-Aldrich, No. T79708), Injection vials (Thermo, lot number: 11190533), Bottle caps (Thermo, lot number: 11150635), Total RNA extraction kit (Solebio, lot number: R1200), Universal reverse transcription kit (Yisheng Bio, lot number: 11141ES60), Realtime PCR real-time quantitative kit (Yisheng Bio, lot number: 11201ES08), BCA protein concentration determination kit (Solarbio, lot number: PC0020), skim milk powder (BD, lot number: 232100), TEMED (Amresco, lot number: Amresc00761), HCl (Xinyang Chemical Reagent Factory, lot number: GB622-89), SDS (Sinopharm, lot number: 30166428), 30% gel solution (Solarbio, lot number: A1010), Tris (Sinopharm, lot number: 30188216), Glycine (Sinopharm, lot number: 62011519), Methanol (Sinopharm, lot number: 10014118), NaCl (Sinopharm, lot number: 10016318), KCl (Sinopharm, lot number: 10020318), Na₂HPO₄·12H₂O (Sinopharm,

lot number: 10017618), KH₂PO₄ (Sinopharm, lot number: 10019718), RIPA lysis buffer (Beyotime, lot number: P0013B), Protein phosphatase inhibitor mixture (Beyotime, lot number: P1045), 5× SDS-PAGE protein loading buffer (Beyotime, lot number: P0015L), Protein marker (thermo, lot number: 26617), PVDF membrane (Millipore, lot number: IPVH00010), ECL luminescent reagent (Beyotime, lot number: P0018S-2), Membrane regeneration solution (Beijing Puli Lai Gene Technology Co., Ltd., lot number: P1650), FGA (Affinity, lot number: DF7895), Human articular chondrocytes (immortalized) (Xiamen ImmoCell Biotechnology Co., LTD, lot number: IM-H488).

Instrumentation and equipment

RIGOL L-3000 High Performance Liquid Chromatography System (Beijing Puyuan Jingdian Technology Co., Ltd.), vortex mixer (SCILOGEX, model: MX-S), vacuum centrifugal concentrator (Beijing Jiai Mother Technology Co., Ltd., model: CV100-DNA), electric heating water bath (Beijing Guangming Medical Instruments Co., Ltd., model: XMTD-7000), centrifuge (Eppendorf), microplate reader (DR200B), electrophoresis system (bio-rad), high-throughput tissue homogenizer (Shanghai Hefan Instruments Co., Ltd., model: hf-48), ultrasonic homogenizer (Shanghai Huxi Industrial Co., Ltd., model: JY96-IIN), 10 K ultrafiltration tube (Sartorius, PN: VN01H02). Benchtop low-speed centrifuge (Shanghai Medical Instruments, model: 80-2), real-time fluorescent quantitative PCR instrument (Molarray, model: MA-6000), nucleic acid detection instrument (Lifereal, model: F-1100), Electrophoresis instrument (Bio-rad, model: 1645070), electroporation instrument (Bio-rad, model: BE6085), pH meter (Mettler-Toledo GmbH, model: LP115), microplate reader (Biotek, model: 800TS), and fully automatic chemiluminescence image analysis system (Tanon, model: 5200).

Protein extraction and mass spectrometry analysis

Label-free quantitative proteomic analysis was performed to investigate differential protein expression between OA and control cartilage. Cartilage samples in the OA group were obtained from the knee joints of OA patients undergoing TKA, while control samples were obtained from the non-load-bearing regions of irreparable cartilage fragments excised during surgical management of tibial plateau fractures. Immediately post-collection, tissues were snap-frozen in liquid nitrogen and cryogenically pulverized into fine powder. Proteins were extracted by adding lysis buffer containing protease inhibitors (50:1, v/v) to the cartilage powder. Homogenates were vortexed and subjected to ultrasonication (1 s on/off pulses, a total of 5 min). Following centrifugation at 14,000 g for 20 min, the supernatant containing soluble proteins

was collected. Protein concentration was quantified using the Bradford assay. Prior to analysis, samples were appropriately diluted with lysis buffer to ensure that their final concentrations fell within the range of the standard curve. Bovine serum albumin (BSA) standards were also prepared in lysis buffer at a series of known concentrations. Then, 10 µL of each sample or standard was mixed with 300 µL of Bradford reagent. After 10-min incubation in the dark, absorbance at 595 nm was measured using a microplate reader. A standard curve was generated from the absorbance values of the BSA standards, and sample concentrations were calculated accordingly. For digestion, 20 µL of each protein extract was incubated with MMB magnetic beads at 37 °C for 30 min, followed by the addition of 45 µL binding buffer and a 15-min incubation with gentle shaking at room temperature. The supernatant was removed, and the beads were washed three times with washing buffer, resuspended in 20 µL of digestion buffer, and incubated at 37 °C for ≥ 4 h. Enzymatic activity was terminated with 5 µL quenching buffer. Digested peptides were lyophilized prior to liquid chromatography-tandem mass spectrometry (LC-MS/MS) analysis. Mobile phases were prepared as follows: Solution A—100% H₂O with 0.1% formic acid; Solution B—80% acetonitrile with 0.1% formic acid. Lyophilized peptides were reconstituted in 10 µL of Solution A, centrifuged at 14,000 g for 20 min at 4 °C, and 1 µg of the supernatant was injected. LC-MS/MS was performed on an Orbitrap Eclipse™ mass spectrometer coupled with a FAIMS Pro™ interface. Compensation voltage alternated between -45 V and -65 V every 1 s. Peptides were ionized *via* a Nanospray Flex™ (NSI) source at 2.0 kV, with an ion transfer tube temperature of 320 °C. The instrument operated in data-dependent acquisition mode. MS1 spectra were acquired in the range of *m/z* 350–1500 at a resolution of 120,000 (*m/z* 200), automatic gain control (AGC) target of 4×10^5 , and max C-trap injection time of 50 ms. MS2 scans were acquired using Top Speed mode with a resolution of 15,000, AGC target of 5×10^4 , max injection time of 22 ms, and normalized collision energy of 33%. Raw data files (.raw format) were generated. Protein identification was conducted using Proteome Discoverer (v2.4) against the UniProt Homo sapiens reference proteome (20,407 entries; downloaded on March 7, 2023).

Quantitative real-time polymerase chain reaction (qPCR) and Western blots validation

We used human articular chondrocytes (immortalized) to the third generation for experimental verification. Chondrocytes were divided into four groups, and normal chondrocytes were the blank control group. The OA chondrocyte models were established by stimulating normal chondrocytes with IL-1β (1 ng/mL) for 24 hours

as the OA model group. After normal chondrocytes were transfected with the negative control fragments for 24 hours and then stimulated with IL-1 β (1 ng/mL) for 24 hours, they became the negative control interference group of the OA models. After normal chondrocytes were transfected with the target gene FGA interference fragments (sense 5'-CCUCAGCCAAUAACCGUGAUA TT-3' and antisens 5'-UAUCACGGUUAUUGGCUGAG GTT-3') for 24 h, they were stimulated with IL-1 β (1 ng/mL) for 24 h to form the target gene interference group of the OA models. Three samples were randomly selected from each of the four groups respectively and verified by Quantitative real-time polymerase chain reaction (qPCR) and western blots.

The experimental process of qPCR

Total RNA was extracted using 1 mL of TRIzol reagent samples of each group. Following phase separation with 0.2 mL chloroform, samples were vortexed for 15 s, incubated at room temperature for 5 min, and centrifuged at 12,000 rpm for 10 min at 4 °C. The aqueous phase was mixed with 200 μ L of anhydrous ethanol and applied to a silica column. After binding for 2 min, the column was washed with 500 μ L of wash buffer and eluted with 50 μ L RNase-free ddH₂O. To remove genomic DNA, RNA was treated with 3 μ L of 5 \times gDNA Digester Mix, 0.5 μ L of primer mix (U6-R(rt)), and 1.5 μ L of RNase-free water, using 10 μ L of RNA as a template in a total reaction volume of 15 μ L. Reverse transcription was performed using 5 μ L of 4 \times Hifair[®] III SuperMix Plus with the following conditions: 25 °C for 5 min, 55 °C for 15 min, and 85 °C for 5 min. The resulting cDNA was diluted 1:10 for subsequent qPCR analysis. Each 20 μ L qPCR reaction included 10 μ L Hieff[®] qPCR SYBR Green Master Mix, 0.5 μ L each of forward and reverse primers, 5 μ L diluted cDNA, and 4 μ L nuclease-free water. Thermal cycling was performed according to standard protocols, including stages of pre-denaturation, denaturation, annealing, and extension. Fluorescence signals were captured in real time by the qPCR instrument, and subsequent quantification was conducted using integrated software. Primer sequences used in qPCR are shown in Table 1. qPCR results were analyzed using the $2^{-\Delta\Delta CT}$ method (Livak method). All qPCR results were analyzed and visualized using Graph-Pad Prism (v 9.5.0).

Table 1 Primer sequences used in qPCR

		Sequence (5'-3')	Length (bp)
GAPDH(h)	F	TCAAGAAGGTGGTGAAGCAGG	21
	R	GCGTCAAAGGTGGAGGAGTG	20
h-FGA	F	CACATTGTCTGGCATAGTACTCTGG	26
	R	TCTCCTCTGTTGTAACCTGCTACT	26

The experimental process of western blots

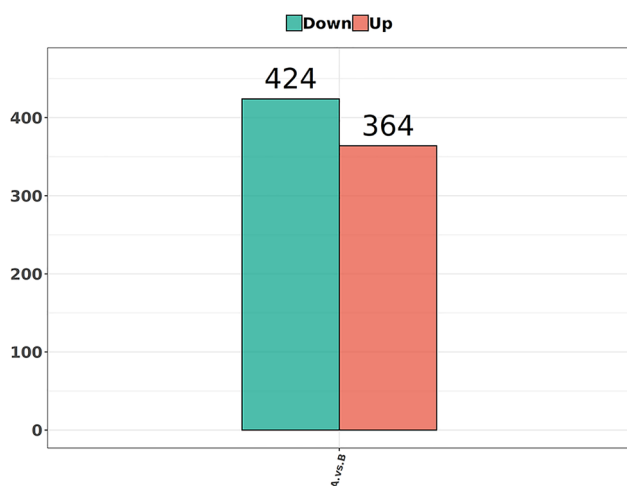
After washing with PBS, each sample was added to the lysis solution and placed on ice for 20 min. The lysate was centrifuged at 12,000 rpm at 4 °C for 20 min and the supernatant was taken. Protein concentration was quantified with a BCA kit; 5 \times loading buffer and PBS were then added to equalize the concentrations across groups. Samples were boiled at 95 °C for 5 min, and 10 μ g of total protein per lane were loaded onto a 10% SDS-PAGE gel. After electrophoresis and transfer to a PVDF membrane, blocking was performed in TBST + 5% skim milk (2 h, room temperature). The membrane was incubated overnight at 4 °C with primary antibodies diluted in TBST + 2% BSA-FGA (rabbit polyclonal, 1: 2000) followed by three 10 - min TBST washes and a 1 h room temperature incubation with HRP-conjugated goat anti-rabbit IgG (1: 5000) before ECL detection. Mixed the enhancing solution in the ECL reagent with the stable peroxidase solution in a 1:1 ratio, added an appropriate amount of working solution onto the PVDF membrane, and exposed it using the fully automatic chemiluminescence image analysis system. After the exposure was completed, thoroughly washed the PVDF membrane with TBST three times, 5 min each time. Added an appropriate amount of membrane regenerant, immersed the PVDF membrane in the membrane regenerant, and eluted it in a shaker at room temperature for 20 min. After that, washed off the excess membrane regeneration liquid. Sealed again and incubated with internal references glyceraldehyde-3-phosphate dehydrogenase (GADPH) (1:5000). HRP-labeled secondary antibody was added again and the exposure was carried out using the fully automatic chemiluminescence image analysis system. The results were analyzed using Image J software to analyze the gray values.

Statistical analysis

Raw proteomic data were processed and analyzed using R software (v4.3.3). Student's t-test was applied to identify differentially expressed proteins between OA and control groups. Proteins with $P < 0.05$ and fold change > 1.5 were considered statistically significant. Functional annotation and enrichment analyses were conducted using Clusters of Orthologous Groups (COG), Gene Ontology (GO), and the Reactome pathway database. To identify central pathogenic candidates, protein-protein interaction (PPI) networks were constructed. Clinical data and validation experiment data, count data were expressed as percentages and cases, and chi-square test was used for comparison between groups. Measurement data were expressed as (Mean \pm SD). If the data conformed to a normal distribution, Student's t-test was used. Conversely, non-parametric tests were used. $P < 0.05$ indicates a statistically significant difference.

Table 2 Clinical data of the enrolled patients

Group	Age (years)	Gender		BMI	Diagnosis	Surgical procedure
		Male	Female			
OA group (n=15)	65.67 ± 3.5	6	9	28.61 ± 2.16	OA	TKA
Control group (n=11)	62.5 ± 2.66	6	5	27.32 ± 3.32	Tibial plateau fracture	ORIF
-	P > 0.05	P > 0.05		P > 0.05	-	-

**Fig. 1** Bar chart illustrating the number of differentially expressed proteins identified between groups. **A:** Control group; **B:** Osteoarthritis (OA) group

Results

Clinical data of the enrolled patients

A total of 26 patients were enrolled in this study, including 15 patients in the OA group and 11 patients in the control group. The OA group comprised 9 females and 6 males with an average age of 65.67 ± 3.5 years, while the control group 5 females and 6 males with an average age of 62.5 ± 2.66 years. The average Body Mass Index (BMI) of patients in the OA group was 28.61 ± 2.16 , and that of patients in the control group was 27.32 ± 3.32 . Patients in the OA group underwent TKA, whereas those in the control group were treated with arthroscopically assisted ORIF. Demographic and surgical details for both groups are summarized in Table 2. There was no statistical significance in the comparison of age, gender and BMI between the two groups ($P > 0.05$). In the OA group, specimens were obtained from degenerated, weight-bearing articular surfaces during TKA procedures. In the control group, cartilage was harvested from non-load-bearing regions that were deemed irreparable during ORIF. Macroscopic examination revealed that OA cartilage displayed surface irregularities, yellowish discoloration, and reduced elasticity, consistent with degenerative matrix remodeling. In contrast, control cartilage appeared smooth, grayish-white, and retained normal biomechanical properties.

Identification of differentially expressed proteins

A total of 788 proteins were identified as differentially expressed between osteoarthritic and control cartilage tissues, with 364 upregulated and 424 downregulated in the OA group (Fig. 1). The complete list of differentially expressed proteins is provided in supplementary material.

Function enrichment analysis

COG analysis

COG analysis categorized the differentially expressed proteins into different functional groups. The most enriched category included proteins involved in post-translational modifications, protein turnover, and chaperone activity (152 proteins). Signal transduction mechanisms accounted for 137 proteins, followed by general function (112), translation, ribosomal structure, and biogenesis (91), and intracellular trafficking, secretion, and vesicular transport (90). Additional categories included cytoskeleton structure (72 proteins), immune defense mechanisms (50), RNA processing and modification (47), energy production and conversion (47), extracellular structure (44), carbohydrate transport and metabolism (42), and amino acid transport metabolism (35) (Fig. 2).

GO enrichment analysis

GO enrichment revealed that differentially expressed proteins were predominantly associated with cellular components (Fig. 3).

Reactome pathway analysis

Reactome pathway analysis revealed that the differentially expressed proteins were significantly enriched in pathways central to cartilage homeostasis and OA progression, including the regulatory signaling pathway of insulin-like growth factor-binding protein (IGFBP) for insulin-like growth factor (IGF) transport and uptake, post-translational protein phosphorylation, and platelet degranulation. Additional pathways of interest included extracellular matrix proteoglycan turnover, complement cascade regulation, extracellular matrix degradation, collagen biosynthesis and modification, and activation of the terminal complement pathway (Fig. 4).

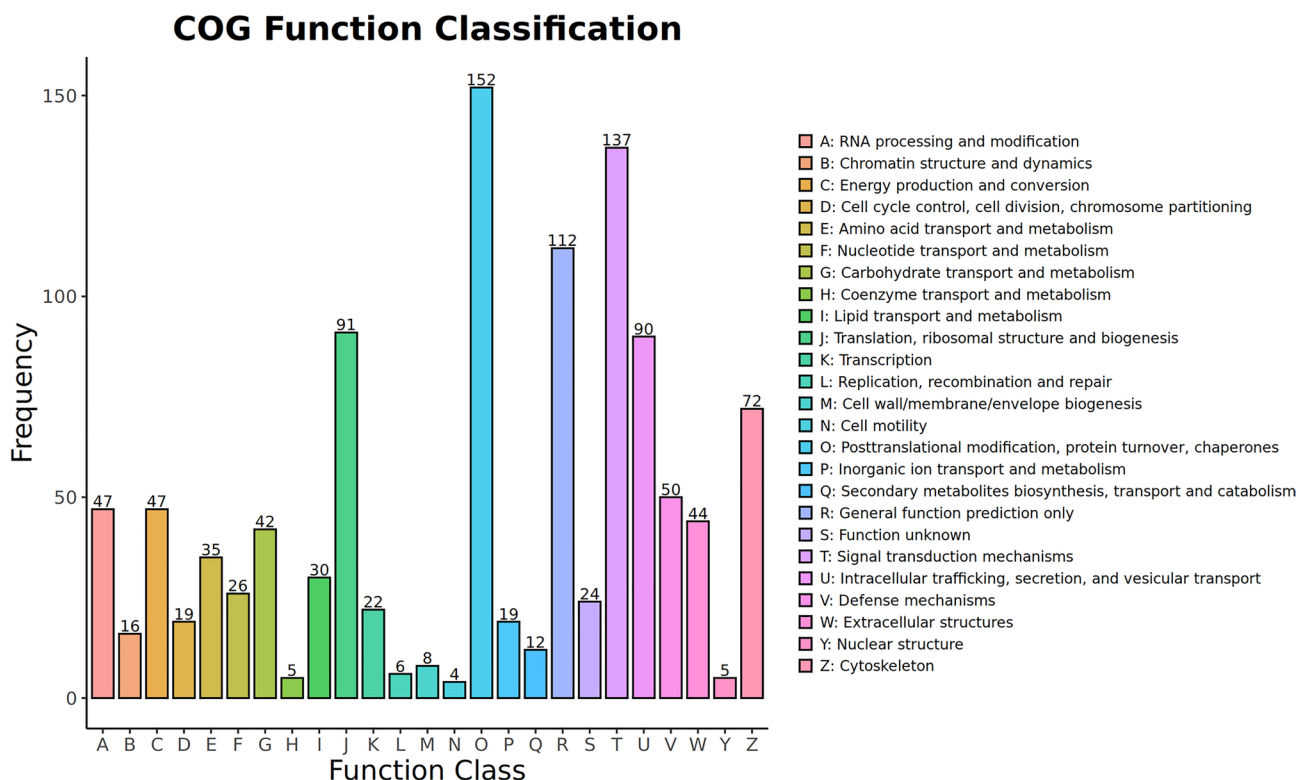


Fig. 2 Functional classification of differentially expressed proteins based on the Clusters of Orthologous Groups (COG) database. Note: The x-axis represents functional categories, the y-axis indicates the number of proteins assigned to each category, and color coding distinguishes different COG terms

PPI network analysis

A PPI network was constructed using differentially expressed proteins. This analysis revealed several hub proteins (genes) with potential relevance to the pathogenesis of OA, including FIBA (*FGA*), FINC (*FNI*), PLMN (*PLG*), APOA1 (*APOA1*), Albumin (*ALB*), ANT3 (*SERPINC1*), FETUA (*AHSG*), FIBG (*FGG*), RL3 (*RPL3*), Apolipoprotein B (*APOB*), CTNB1 (*CTNBN1*), ITB1 (*ITGB1*), KPYM (*PKM*), CD44 (*CD44*), HPT (*HP*), THRB (*F2*), TPIS (*TPI1*), RL5 (*RPL5*), G3P (*GAPDH*), RS16 (*RPS16*), and CXCL7 (*PPBP*) (Fig. 5).

Identification of the key pathogenic protein

Reactome pathway analysis of the differentially expressed proteins identified that the regulatory signaling pathway of IGFBP for IGF transport and uptake and the platelet degranulation signaling pathway were key signaling pathways involved in the pathogenesis of OA. From these two pathways, 89 related genes were identified as significantly involved (Figs. 6 and 7). In these two key signaling pathways, fibrinogen alpha chain (*FGA*) in the OA group was highly expressed. Moreover, in the PPI network analysis, FIBA, encoded by *FGA*, was also the hub protein in the pathogenesis of OA. Therefore, by integrating the results of PPI network analysis and pathway enrichment, *FGA*, is the key pathogenic gene involved in OA.

Validation of *FGA* expression in OA by qPCR

In the qPCR analysis, amplification curves demonstrated characteristic sigmoidal shapes, and melting curves showed single peaks (the amplification curves and melting curves can be found in the supplementary materials). The results of qPCR showed that the expression of *FGA* mRNA in OA group and the negative control interference group of the OA models was much higher than that in other groups (Fig. 8). This result confirmed that *FGA* was highly expressed in OA chondrocytes.

Validation of *FGA* expression in OA by Western blots

The western blots results showed that the expression of *FGA* in the OA model group and the OA model negative control interference group was significantly higher than that in the control group, while in the OA model *FGA* interference group, the expression of *FGA* was significantly lower than that in the control group (Figs. 9 and 10). The results of western blots suggested that *FGA* was highly expressed in OA chondrocytes.

Discussion

In this study, knee cartilage tissues from patients with knee OA and normal knee cartilage from patients with knee joint injury were used for comparative proteomics analysis. The results of this study showed that the regulatory signaling pathway of IGFBP for IGF transport and

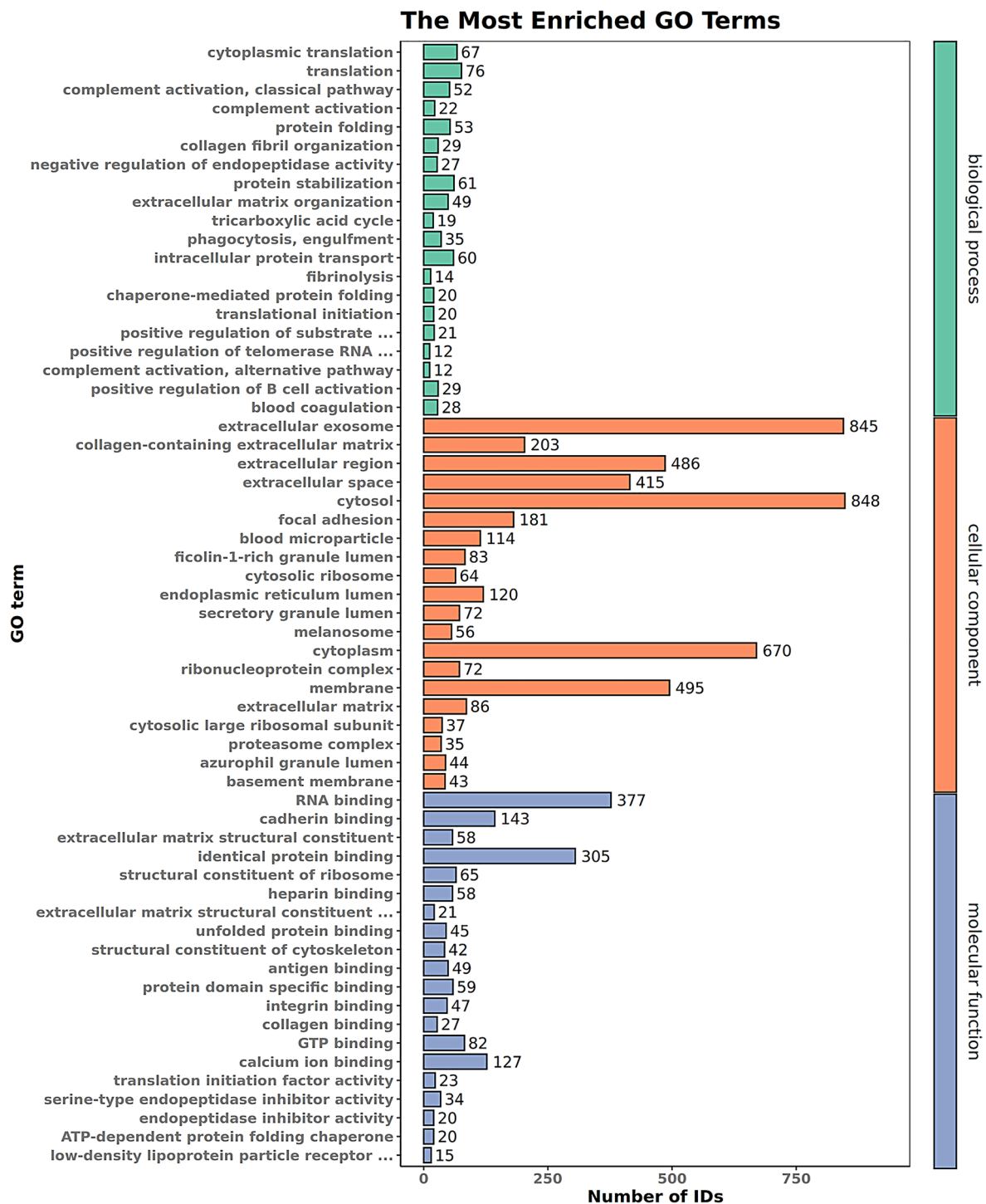


Fig. 3 Gene Ontology (GO) enrichment analysis of differentially expressed proteins. Note: The x-axis displays the number of proteins associated with each GO term, and the y-axis represents the top 20 enriched terms within the three GO domains: Biological Process, Cellular Component, and Molecular Function

uptake and the platelet degranulation signaling pathway were key signaling pathways involved in the pathogenesis of OA. In addition, we identified *FGA* as a key pathogenic gene in OA. These findings were independently validated by qPCR and western blots, confirming elevated *FGA*

expression in OA articular chondrocytes samples compared to controls. To our knowledge, this is the first study to report a mechanistic role for *FGA* in OA pathogenesis [11].

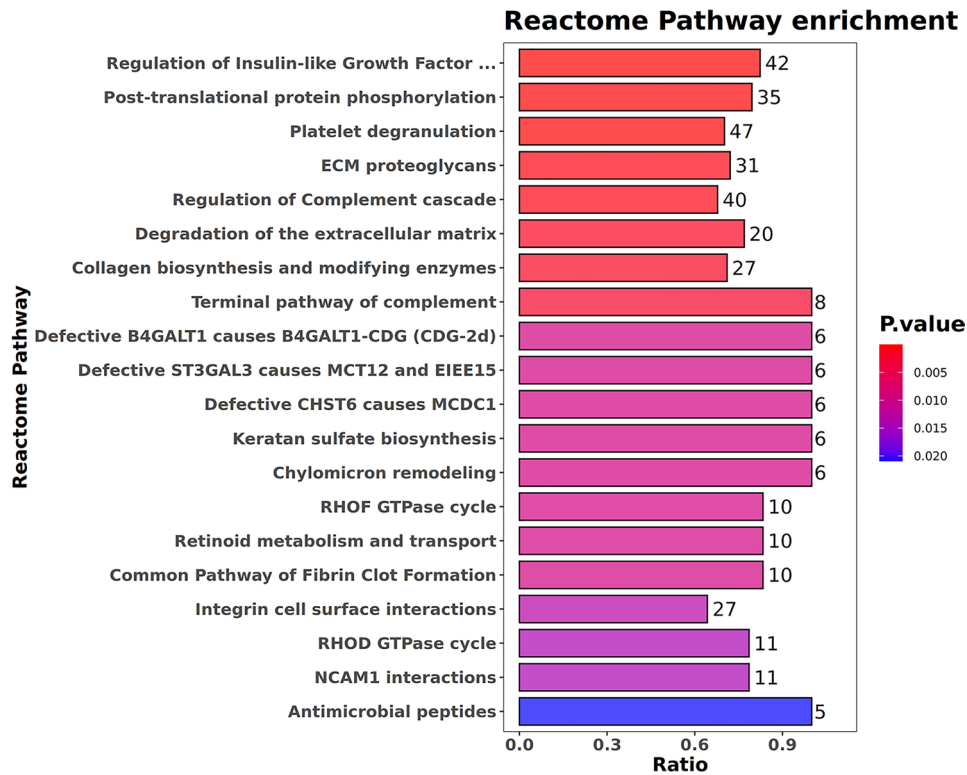


Fig. 4 Reactome pathway enrichment analysis of differentially expressed proteins. Note: The y-axis shows the top 20 enriched pathways ranked by enrichment score (all are listed as the number was fewer than 20). The x-axis represents enrichment ratios, bar color reflects the P-value, and the numeric values indicate the number of proteins enriched in each pathway

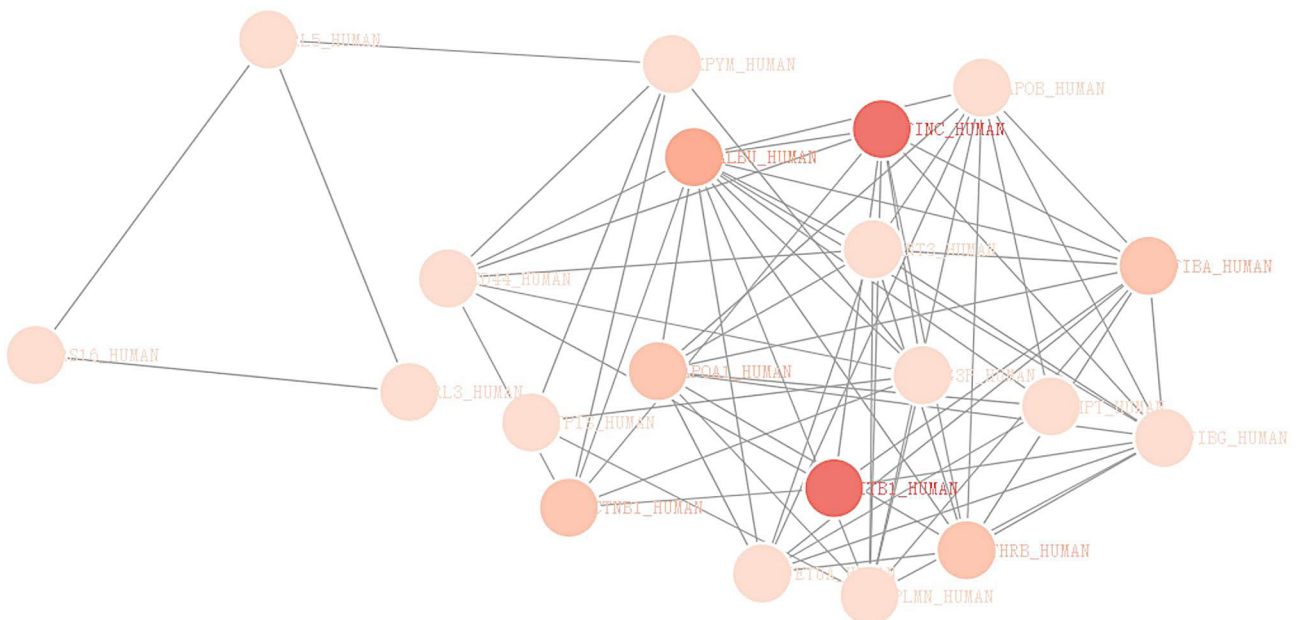


Fig. 5 Protein-protein interaction (PPI) network of differentially expressed proteins. Note: Nodes represent individual proteins, color-coded by expression direction (upregulated or downregulated), and edges indicate predicted or known interactions between proteins

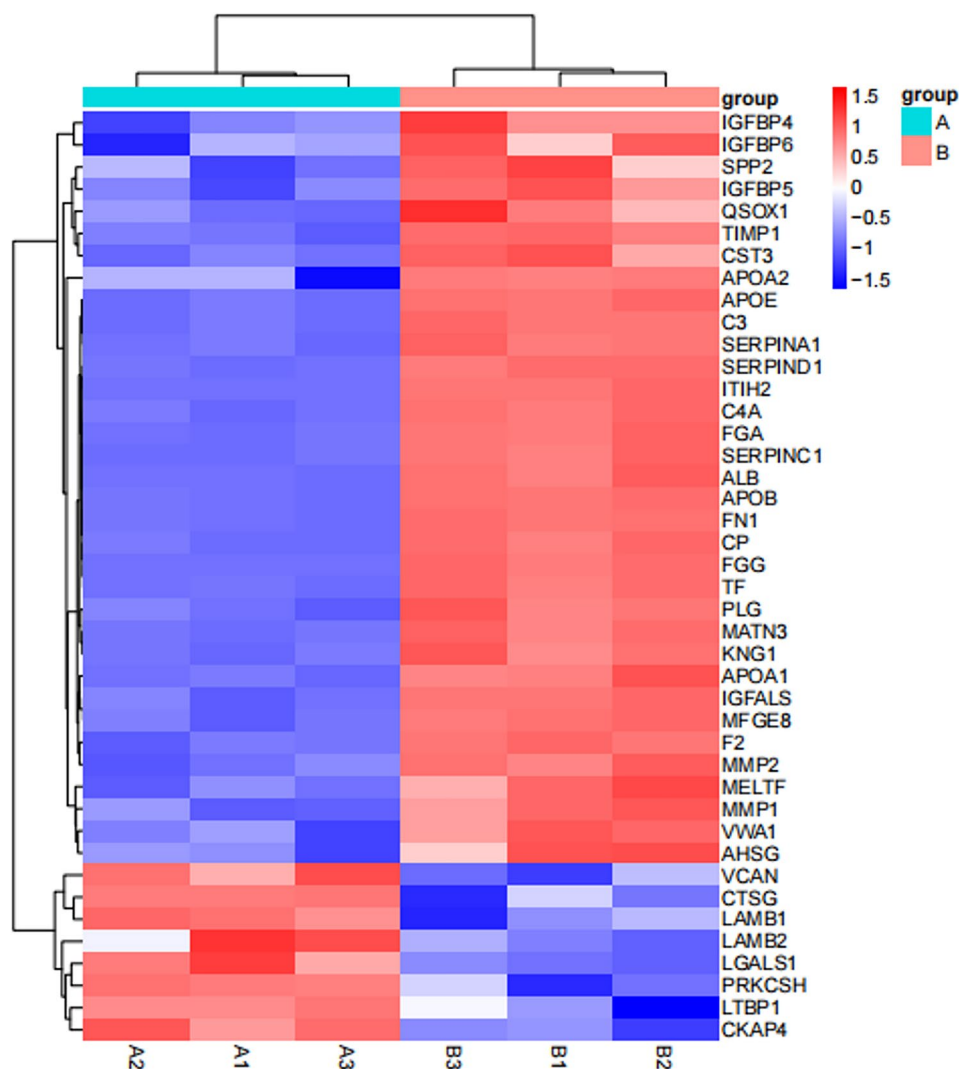


Fig. 6 Heatmap of genes associated with the IGF-binding protein-mediated IGF transport and uptake signaling pathway. Note: Hierarchical clustering reveals distinct molecular signatures between the OA and control groups. The x-axis represents individual samples, and the y-axis lists the corresponding differentially expressed proteins. The color gradient reflects relative expression levels, with red indicating high expression and blue indicating low expression. **A:** Control group; **B:** Osteoarthritis (OA) group

Fibrinogen, an important component of blood coagulation, is transformed into fibrin net by thrombin catalysis in the circulatory system, leading to coagulation and hemostasis [12]. Fibrinogen molecule is composed of three polypeptide chains: $\text{A}\alpha$, $\text{B}\beta$, and γ . The *FGA* gene encodes the $\text{A}\alpha$ chain, which is critical for thrombin-mediated fibrin clot formation. Mutations or dysregulation of *FGA* have been associated with coagulation disorders, such as afibrinogenemia, hypofibrinogenemia, and renal amyloidosis [13]. In this study, *FGA* expression was upregulated in OA cartilage tissue of patients with OA, which has not been reported previously. In addition, *FGA* was highly expressed in the regulatory signaling pathway of IGFBP for IGF transport and uptake and the platelet degranulation signaling pathway in this study.

Reactome pathway analysis found that the regulatory signaling pathway of IGFBP for IGF transport and uptake played an important role in the pathogenesis of OA. IGF is an important growth factor regulated by IGFbps. Thus far, six different IGFbps have been identified [14]. When IGFbps bind to IGF, they form a stable complex. Upon reaching the target tissue, IGFbps are enzymatically cleaved, releasing free IGF, which can then interact with its receptor to promote the growth of the target organ cells [15]. Among the IGFBP family, IGFBP-5 plays a particularly important role in regulating IGF release in tissues such as bone, cartilage, and muscle, hereby influencing the growth and differentiation of these tissues [16]. Therefore, we conclude that the dysregulation of IGFBP-mediated IGF transport and uptakes stimulates the abnormal proliferation of chondrocytes at the

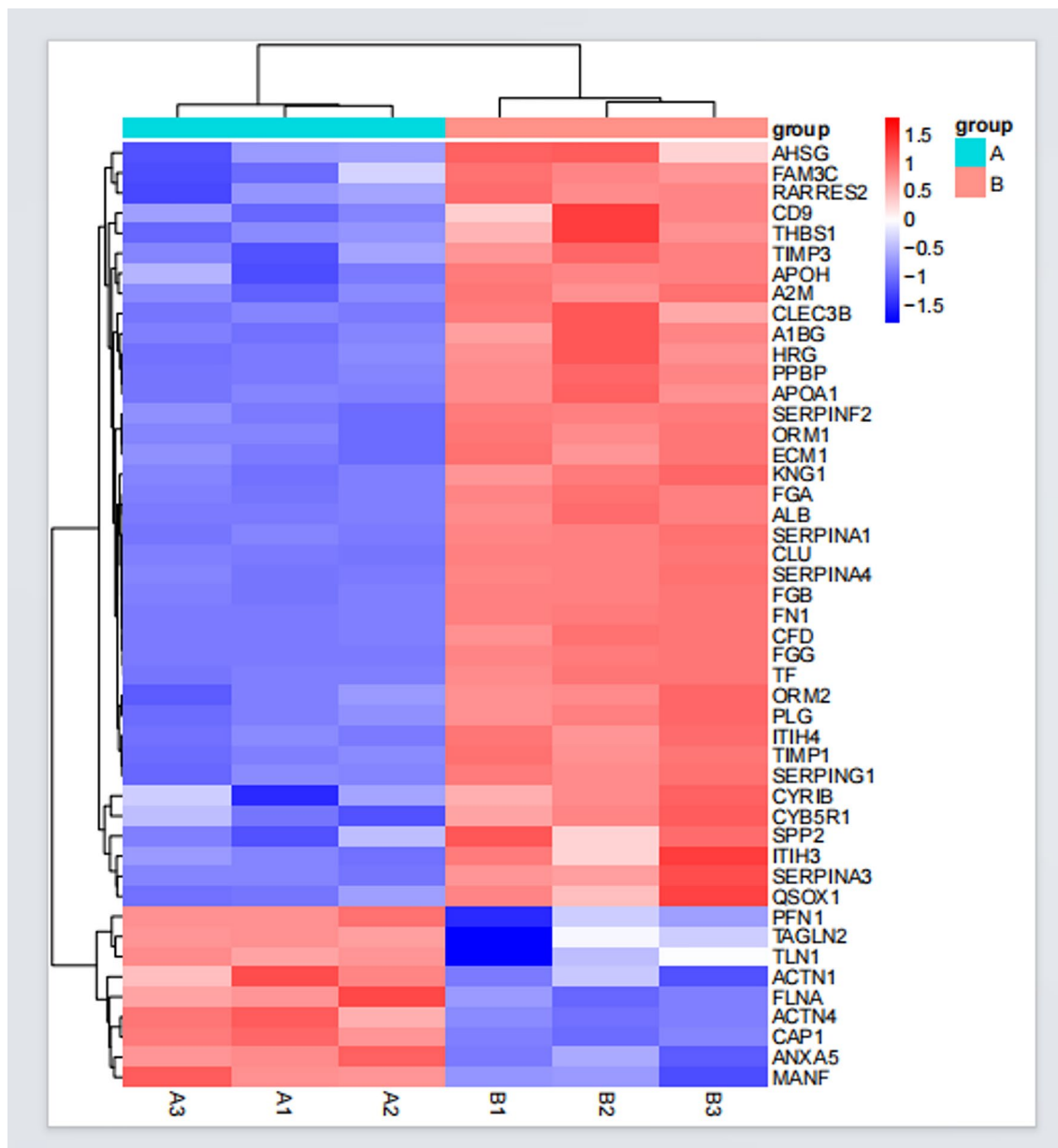


Fig. 7 Heatmap of genes involved in the platelet degranulation signaling pathway. **A:** Control group; **B:** Osteoarthritis (OA) group

focal site of OA patients, thereby causing cartilage tissue hyperplasia.

Reactome pathway analysis also identified the platelet degranulation signaling pathway as a potentially important contributor to the pathogenesis of OA. Platelet degranulation refers to the release of bioactive molecules, including platelet factors and growth factors, from intracellular granules into the external environment. These molecules play critical roles in coagulation, inflammation, and vascular repair [17]. Platelet activation is mediated by many receptors, including phosphatidylinositol triphosphate receptors (IP3Rs), phosphatidylinositol tetrakisphosphate receptors (IP4Rs), and G protein-coupled

receptors. Activation of these receptors triggers downstream signaling pathways, such as the phosphatidylinositol signaling pathway, protein kinase C (PKC) signaling pathway, and RhoA/ROCK signaling pathway. The RhoA / ROCK signaling pathway can also lead to articular cartilage degeneration by remodeling the microfilament cytoskeleton of chondrocytes [18].

Enrichment analyses revealed that *FGA* is involved in multiple key pathways associated with OA, including the regulatory signaling pathway of IGFBP for IGF transport and uptake and the platelet degranulation signaling pathway. However, at present, no relevant targeted therapies have been identified. Given *FGA*'s central involvement

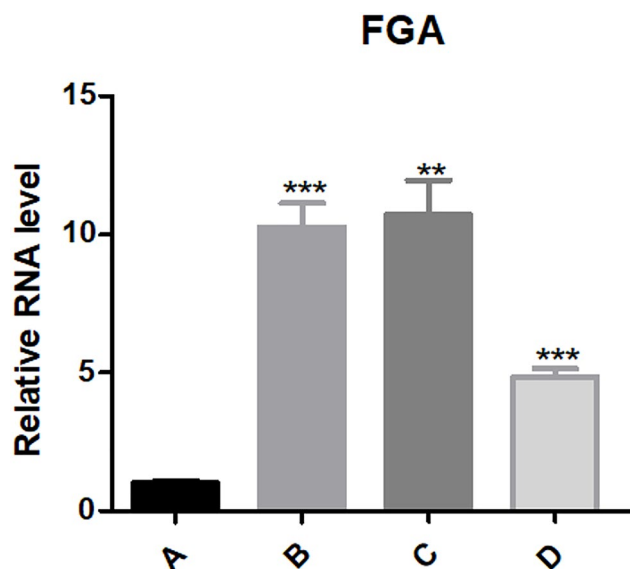


Fig. 8 Relative expression of *FGA* in cartilage samples under different experimental conditions. (A) Control group; (B) OA group; (C) the negative control interference group of the OA models; (D) The *FGA* interference group of the OA models. Note: *Significant differences ($P < 0.05$); **Very significant differences ($P < 0.01$); ***Extremely significant differences ($P < 0.001$)

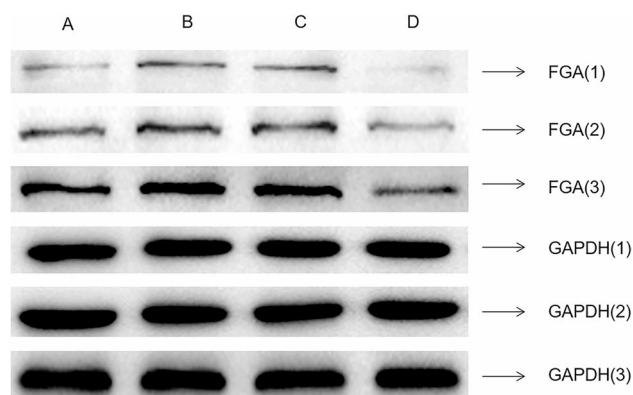


Fig. 9 The band charts of western blots. (A) Control group; (B) OA group; (C) the negative control interference group of the OA models; (D) The *FGA* interference group of the OA models

in both the IGFBP regulatory signaling pathway for IGF transport and uptake and the platelet granulation signaling pathway, we searched the Drugbank database (<https://go.drugbank.com/>) and identified 17 drugs targeting the *FGA* [19]. These drugs include alteplase, reteplase, anistreplase, tenecteplase, alimpeprase, ancrod, EP-2104R, lanoteplase, prothrombin, anti-inhibitor coagulant complex, zinc, thrombin alfa, human thrombin, thrombin, zinc acetate, zinc chloride, and zinc sulfate. These findings suggest that zinc acetate, zinc chloride, and zinc sulfate inhibit the expression of *FGA*, which indicates the inhibitory effect of zinc on *FGA*.

This study has several limitations. First, the sample size was relatively small, which may affect the reliability of the

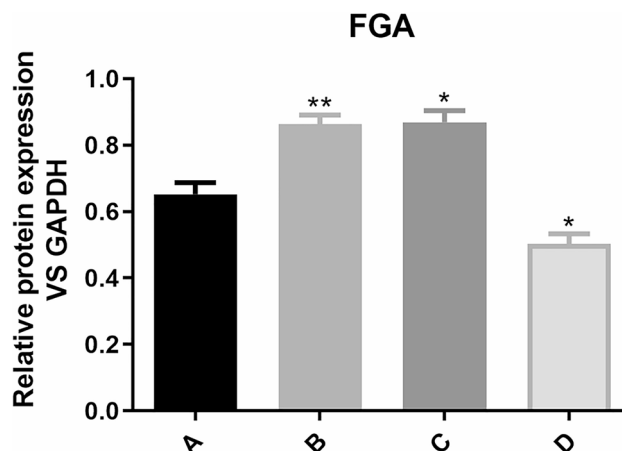


Fig. 10 The results of Western blots. (A) Control group; (B) OA group; (C) the negative control interference group of the OA models; (D) The *FGA* interference group of the OA models. Note: *Significant differences ($P < 0.05$); **Very significant differences ($P < 0.01$); ***Extremely significant differences ($P < 0.001$)

study findings. Second, due to ethical constraints, control cartilage was sourced from non-load-bearing, irreparable areas in patients with tibial plateau fractures rather than from completely healthy individuals. Although these regions appeared morphologically intact, prior trauma may have induced subclinical inflammation, potentially affecting protein expression profiles. Third, the study population was exclusively composed of Chinese patients; further validation is needed to assess applicability across other ethnic groups. Finally, while potential *FGA*-targeting drugs were identified through database screening, no functional or preclinical experiments were conducted. Therefore, future research with larger, multi-ethnic cohorts and functional validation studies is warranted to explore the translational potential of targeting *FGA* in OA treatment.

Conclusions

FGA plays an important role in the pathogenesis of OA, and it can be used as a new target for the development of precision treatments for OA.

Abbreviations

OA	Osteoarthritis
GWAS	Genome-wide association studies
FGA	Fibrinogen alpha chain
TGF	Tumor growth factor
Ihh	Indian Hedgehog
PTHrP	Parathyroid hormone-associated protein
TKA	Total knee arthroplasty
ORIF	Open reduction and internal fixation
BSA	Bovine serum albumin
LC-MS/MS	Liquid chromatography-tandem mass spectrometry
AGC	Automatic gain control
qPCR	Quantitative real-time polymerase chain reaction
SD	Sprague-Dawley
COL-II	Collagen type II
AST	Aspartate Transaminase

ALT	Alanine Transaminase
BMI	Body Mass Index
COG	Clusters of Orthologous Groups
GO	Gene Ontology
PPI	Protein-protein interaction
IGFBP	Insulin-like growth factor-binding protein
IGF	Insulin-like growth factor
PKC	Protein kinase C

Supplementary Information

The online version contains supplementary material available at <https://doi.org/10.1186/s12891-025-08738-1>.

Supplementary Material 1
Supplementary Material 2
Supplementary Material 3
Supplementary Material 4
Supplementary Material 5
Supplementary Material 6
Supplementary Material 7
Supplementary Material 8
Supplementary Material 9

Acknowledgements

The authors thank all the patients for their participation and permission in this study. We thank TopEdit (www.topedit.com) for its linguistic assistance during the preparation of this manuscript.

Author contributions

1)Guanhong Chen and Xizhuang Bai made substantial contributions to the conception or design of the work; Guanhong Chen and Han Zhang made the acquisition, analysis, and interpretation of data; 2) Guanhong Chen, Han Zhang and Xizhuang Bai drafted the work or revised it critically for important intellectual content; 3) Guanhong Chen, Han Zhang and Xizhuang Bai approved the version to be published; 4) Xizhuang Bai agreed to be accountable for all aspects of the work in ensuring that questions related to the accuracy or integrity of any part of the work are appropriately investigated and resolved.

Funding

This research was funded by Young Elite Sponsorship Program of Shandong Provincial Medical Association (Grant ID 2023_LC_0267).

Data availability

The datasets generated and/or analysed during the current study are available in the ProteomeXchange repository, <https://www.iprox.cn/page/SCV017.html?query=PXD063166>.

Declarations

Ethics approval and consent to participate

The study was conducted in accordance with the 1964 Declaration of Helsinki and was approved by the Medical Ethics Committee of Liaoning Provincial People's Hospital in 2022-12-03 (No.2022120316). Informed consent was obtained from all individual participants included in the study.

Consent for publication

Not applicable.

Competing interests

The authors declare no competing interests.

Received: 16 January 2025 / Accepted: 9 May 2025

Published online: 20 May 2025

References

1. Abramoff B, Caldera FE, Osteoarthritis. Pathology, diagnosis, and treatment options. *Med Clin North Am.* 2020;104(2):293–311.
2. Martel-Pelletier J, Barr AJ, Cicuttini FM, et al. Osteoarthritis. *Nat Rev Dis Primers.* 2016;2:16072.
3. Glyn-Jones S, Palmer AJ, Agricola R, et al. Osteoarthritis. *Lancet.* 2015;386(9991):376–87.
4. Giorgino R, Albano D, Fusco S, Peretti GM, Mangiavini L, Messina C. Knee osteoarthritis: epidemiology, pathogenesis, and mesenchymal stem cells: what else is new?? An update. *Int J Mol Sci.* 2023;24(7):6405.
5. Pereira D, Ramos E, Branco J, Osteoarthritis. *Acta Med Port.* 2015;28(1):99–106.
6. Mandl LA. Osteoarthritis year in review 2018: clinical. *Osteoarthritis Cartilage.* 2019;27(3):359–64.
7. Jiang Y. Osteoarthritis year in review 2021: biology. *Osteoarthritis Cartilage.* 2022;30(2):207–15.
8. Xia B, Chen D, Zhang J, Hu S, Jin H, Tong P. Osteoarthritis pathogenesis: a review of molecular mechanisms. *Calcif Tissue Int.* 2014;95(6):495–505.
9. Taruc-Uy RL, Lynch SA. Diagnosis and treatment of osteoarthritis. *Prim Care.* 2013;40(4):821–36, vii.
10. Litwic A, Edwards MH, Dennison EM, Cooper C. Epidemiology and burden of osteoarthritis. *Br Med Bull.* 2013;105:185–99.
11. Bradford MM. A rapid and sensitive method for the quantitation of microgram quantities of protein utilizing the principle of protein-dye binding. *Anal Biochem.* 1976;72:248–54.
12. Risser F, Urosev I, López-Morales J, Sun Y, Nash MA. Engineered molecular therapeutics targeting fibrin and the coagulation system: a biophysical perspective. *Biophys Rev.* 2022;14(2):427–61.
13. Roy S, Sun A, Redman C. In vitro assembly of the component chains of fibrinogen requires Endoplasmic reticulum factors. *J Biol Chem.* 1996;271(40):24544–50.
14. Song F, Zhou XX, Hu Y, Li G, Wang Y. The roles of Insulin-Like growth factor binding protein family in development and diseases. *Adv Ther.* 2021;38(2):885–903.
15. LeRoith D, Holly J, Forbes BE. Insulin-like growth factors: ligands, binding proteins, and receptors. *Mol Metab.* 2021;52:101245.
16. Beattie J, Allan GJ, Lochrie JD, Flint DJ. Insulin-like growth factor-binding protein-5 (IGFBP-5): a critical member of the IGF axis. *Biochem J.* 2006;395(1):1–19.
17. Barendrecht AD, Verhoef J, Pignatelli S, Pasterkamp G, Heijnen H, Maas C. Live-cell imaging of platelet degranulation and secretion under flow. *J Vis Exp.* 2017;(125):55658.
18. Trzeciak-Ryczek A, Tokarz-Deptuła B, Deptuła W. Platelets—an important element of the immune system. *Pol J Vet Sci.* 2013;16(2):407–13.
19. Wishart DS, Feunang YD, Guo AC, et al. DrugBank 5.0: a major update to the drugbank database for 2018. *Nucleic Acids Res.* 2018;46(D1):D1074–82.

Publisher's note

Springer Nature remains neutral with regard to jurisdictional claims in published maps and institutional affiliations.